*31st EPS Conference on Plasma Phys. London, 28 June - 2 July 2004 ECA Vol.**28G**, P-5.158 (2004)*

The Combined Toroidicity, Ellipticity and Triangularity Effects on the Alfvén Modes Excited in Pre-Heated, Low Aspect Ratio Tokamaks: A Systematic Parametric Study

S.Cuperman[1], C.Bruma[1,2] and K.Komoshvili[1,2]
[1] *Tel Aviv University, Ramat Aviv, Israel*
[2] *The College of Judea and Samaria, Ariel, Israel*

Introduction. In non-uniform plasmas, due to degeneracy in the Alfvén eigenmode spectrum, coupling of poloidal harmonics is possible; as a consequence, (i) gaps in the shear Alfvén continuum spectrum emerge, and (ii) discrete global Alfvén eigenmodes with frequencies inside the continuum gaps are generated. These include: 1) Toroidicity-induced gaps and corresponding Alfvén eigenmodes (TAEs); 2) Ellipticity-induced gaps and corresponding Alfvén eigenmodes (EAEs) and 3) Triangularity-induced gaps and corresponding eigenmodes (non-circular Alfvén eigenmodes, NAEs).

In view of the complexity of the problem and, consequently, of the necessity of determining and interpreting these combined effects (global picture, nature of the waves, mode coupling, gaps, eigenmodes) we considered the case of a **pre-heated** low aspect ratio tokamak in the presence of externally (antenna) launched fast waves, mode converted at Alfvén resonance magnetic surfaces. Thus, we studied systematically the case of the low aspect ratio tokamak START (Sykes, 1994; Wilson, 1994). Specifically, we solved rigorously the full $2\frac{1}{2}$D wave equations for the vector and scalar potentials (actually, 16 second order partial differential equations for the real and imaginary parts, in the upper and lower half planes). Next, we carried out a systematic parametric investigation aimed at the physical understanding and modes identification of the results. The results of our investigation clearly indicate that, due to their global structure, the Alfvén eigenmodes induced by the combined plasma non-uniformity features considered in this work (toroidicity, ellipticity and triangularity) may be quite efficient for, e.g., plasma heating, non-inductive current drive and turbulent transport suppression barriers in the pre-heated stage of low aspect ratio tokamaks.

In terms of the vector and scalar potentials $(\mathbf{A}, \Phi)$, with the notation $\mathcal{A} = i\omega\mathbf{A}$, Maxwell's equations can be written in the following conservative form:

$$\frac{\partial}{\partial\theta}\,\mathsf{L} + \frac{\partial}{\partial\rho}\,\mathsf{M} = \hat{\mathsf{F}}\cdot\,\mathsf{U} - \mathsf{H}\ . \tag{1}$$

$$\mathsf{U} \equiv \begin{bmatrix} \mathcal{A}_\rho \\ \mathcal{A}_\theta \\ \mathcal{A}_\phi \\ \Phi \end{bmatrix},\quad \mathsf{H} \equiv -\frac{\rho^2}{k_0^2}\begin{bmatrix} \mathcal{J}_\rho \\ \mathcal{J}_\theta \\ \mathcal{J}_\phi \\ 0 \end{bmatrix},\quad \mathsf{L} = \begin{bmatrix} \mathcal{A}_{\rho,\theta}/k_0^2 \\ \mathcal{A}_{\theta,\theta}/k_0^2 \\ \mathcal{A}_{\phi,\theta}/k_0^2 \\ \mathsf{L}_4 \end{bmatrix},\quad \mathsf{M} = \begin{bmatrix} \rho^2\mathcal{A}_{\rho,\rho}/k_0^2 \\ \rho^2\mathcal{A}_{\theta,\rho}/k_0^2 \\ \rho^2\mathcal{A}_{\phi,\rho}/k_0^2 \\ \mathsf{M}_4 \end{bmatrix}. \tag{2}$$

The matrix-operator $\hat{\mathsf{F}}$ in eq.(1), and the dielectric tensor operator $\hat{\varepsilon}$ entering $\hat{\mathsf{F}}$ have the following structure:

$$\hat{\mathsf{F}} \equiv \mathsf{F}^0 + \mathsf{F}^1 + \mathsf{F}^\theta\frac{\partial}{\partial\theta} + \mathsf{F}^\rho\frac{\partial}{\partial\rho}\quad ,\quad \hat{\varepsilon} \equiv (\varepsilon^0 + \frac{1}{\rho}\varepsilon^\theta\partial_\theta + \varepsilon^\rho\partial_\rho). \tag{3}$$

The explicit expressions of L_4, M_4, F^0, F^1, F^θ F^ρ and ε^0, ε^θ, ε^ρ are given in Cuperman *et al.*, 2003.

The numerical solution of the wave equations was obtained by the aid of a $2\frac{1}{2}$D finite element code PDE2D (Sewell, 1993), conveniently adapted to the present problem. Full details of the analytical+numerical algorithm used as well as of its reliability checks are given in Cuperman *et al.*, 2003 (see Figure 1).

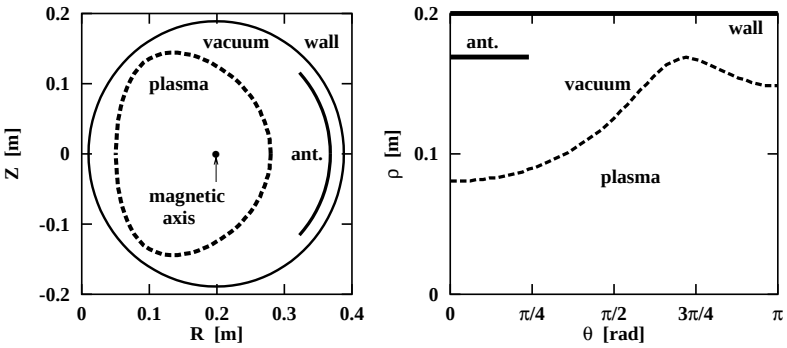

Figure.1 *Right: simulated spherical tokamak configuration; Left: computational configuration.*

General results. Upon carrying out a systematic investigation with respect to the characteristics of the antenna launched FWs (wave frequency as well as toroidal and poloidal wave numbers, N, M) the following general conclusions were found to hold (see Figure 2).

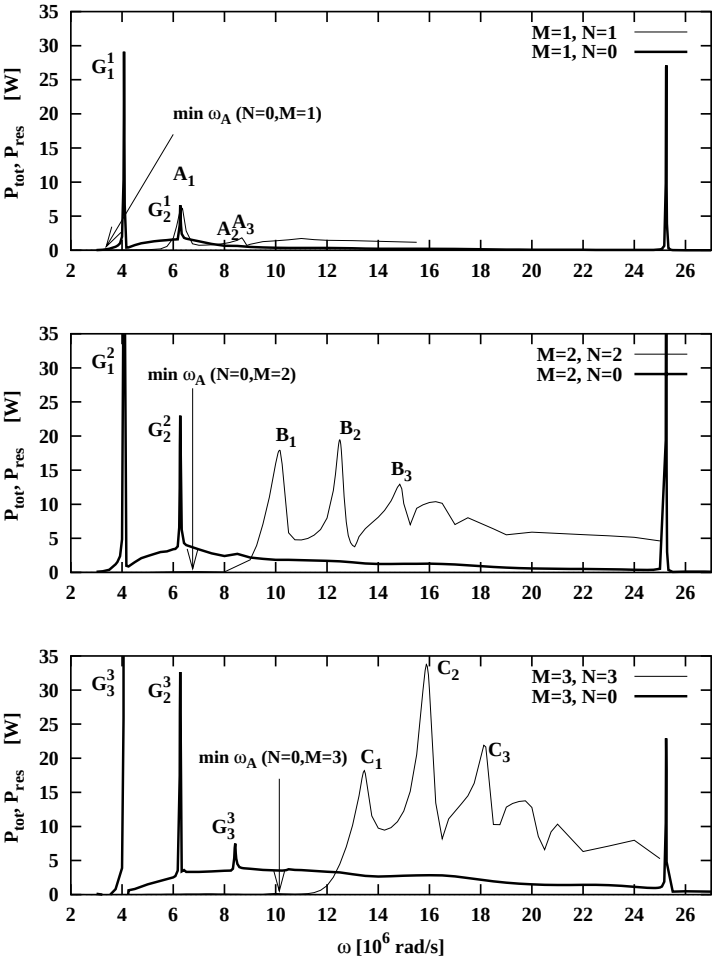

Figure.2 *Comparison of the frequency spectra for $N = 0$ (thick curves) and $N \neq 0$ (thin curves) for the cases $(N = 1, M = 1)$,$(N = 2, M = 2)$ and $(N = 3, M = 3)$. Also indicated are lower-edge of the Alfven continuum values, min ω_A.*

1. In all cases of non-uniformity induced eigenmodes (TAEs, EAEs and NAEs) investigated , total power deposition values significantly larger than those predicted for the Alfvén continuum eigenmodes in a cylindrical plasma were found.

2. With increasing toroidal antenna wave number N, the entire power spectrum — consisting of several peaks — is displaced towards higher frequency values, as well as to higher power peaks values.

3. For $N > 1$, the total deposition power, P_{tot}, is essentially equal to the total resistive power, P_{res}. The situation is different in the case $|N| = 1$: for $N = +1$, P_{tot} differs from P_{res}, thus implying the presence of a significant amount of circulating negative power, $P_{conv} < 0$. When $N = -1$ (not shown here) the relations $P_{tot} \gtrsim P_{res}$, $P_{conv} \ll P_{res}$ hold.

Comparison of the frequency spectrum with that predicted for cylindrical, circular cross-section plasmas. The simplest theoretical ideal MHD model approximates the toroidal axisymmetric plasma of major radius R by a cylindrical, circular, current carrying plasma column with periodicity $2\pi R$ ($k = n/R$); then, the safety factor q defined as the inverse rotational transform of the magnetic field over a length $2\pi R$ is $q = rB_z/RB_\theta$. The wave equation corresponding to this model describes the fast magnetosonic wave and the Alfvén wave; the latter has a spectrum including two types of eigenmodes — a continuum and a discrete set of eigenmodes (which include GAE's, global Alfvén eigenmodes, essentially due to the magnetic shear) (Appert and Vaclavik, 1983). The continuum frequencies (i) are proportional to $|m|$ and (ii) for $n = 0$, there are no crossings of continua for different m-values, and therefore toroidal coupling cannot create gaps and TAE's in the continuum.

Thus, we solved eqs.(1)–(3) for $N = 0$ and $M = 1, 2, 3$ and present the results in Figure 2, together with the general ($N \neq 0$) ones. As seen, the changes in the structure of power spectrum brought up by the plasma nonuniformity, are quite dramatic.

Analysis of toroidicity, ellipticity and triangularity effects. While the prediction of the simple cylindrical plasma model of the possible existence of the crossings of pairs of poloidal modes $(k_{\parallel,m},\ -k_{\parallel,m+1})$, $(k_{\parallel,m},\ -k_{\parallel,m+2})$ and $(k_{\parallel,m},\ -k_{\parallel,m+3})$ consistent with the actual safety factor profile, as well as of the corresponding frequency ratios 1:2:3 are indeed confirmed, their predicted spectral location is a factor of about two lower than shown in Figure 2. However, as shown in Figure 3, when the more general theory, which takes into account the plasma non-uniformity, is used for the evaluation of the global eigenmodes frequencies and gaps, a satisfactory agreement is obtained; this, inspite of the fact the the theory strictly holds for large aspect ratio ($R/a \gg 1$).

Thus, the rigorous results obtained in this work confirm qualitatively the basic theoretical predictions of the inherently simpler and approximate analytical models. They may be useful for the understanding and interpretation of the experimental observations as well as for the planning — upon carring out optimization-oriented computations along lines followed in this work — of different r.f. heating or other r.f. connected experiments, for a similar ST-stage. Finally, this work provides the necessary confidence for extending it to higher temperature regimes, by incorporation of additional appropriate contributions (viz., kinetic and trapping effects) to the quite general dielectric tensor operator used here.

While the qualitative explanation of the rigorous computational results obtained and presented in Figure 2, in terms of inherently simple theoretical models is satisfactory, **some quantitative aspects are still open**; presumably, the classification of the modes according to the poloidal numbers M made by analogy with the cylindrical case does not necessarily represent the actual situation in a START-like device.

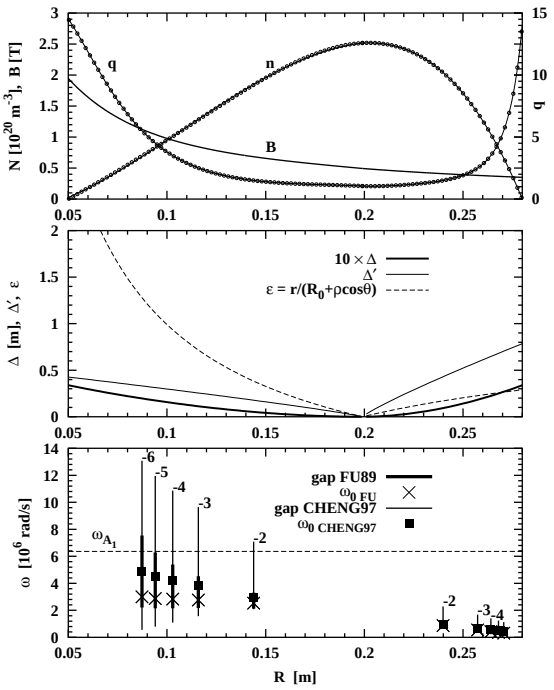

Figure.3 *Theoretically predicted TAE gaps and eigenmodes corresponding to the peak ω_{A_1} in Figure 2 ($N = 1, M = 1$). Top: radial profiles of the magnetic field, electron density and safety factor in the $Z = 0$ plane. Middle: Shafranov shift, Δ, its derivative Δ' and the local toroidal coupling factor $\epsilon_0 = r_0/R$ at positions satisfying the TAE coupling condition, consistent with START's $q(r)$. Bottom: frequency width of the TAE-gaps calculated with Fu, 1989 model (thick lines) and with the more general Cheng 1997 model (thin lines); the squares (crosses) indicate the location of the TAE-eigenmodes according to Cheng 1997 (crossing points where $k_{\|m} = -k_{\|m+1}$) theory; the dashed line indicates the exact numerical value ω_{A_1}. (The numbers $-2, .., -6$ attached to the gaps widths represent the corresponding poloidal wave numbers m of the exited modes which are consistent with the TAE-coupling conditions in START)*

The same applies also to the simple picture of relatively narrow, well separated spectral distances of the non-uniformity induced gaps and eigenmodes, implying (i) a weak coupling of a pair of poloidal harmonics and (ii) circular outermost flux magnetic surface. The more realistic case should also include processes such as: (i) multi-wave interactions, (ii) interaction of gaps of the same kind (all toroidicity induced) and of different kinds (toroidicity, ellipticity, etc – induced) and (iii) secondary or higher order gaps arising when each of a pair of modes is coupled to one or other modes through some other coupling parameters. Moreover, the actual D-shaped topology of all magnetic flux surfaces, including the outermost one, should be taken into account.

References

[1] Appert, K. and Vaclavik, J. 1983 *Plasma Physics* **25**, 551.

[2] Betti, R. and Freidberg, J.P. 1992 *Phys. Fluids* **B4**, 1465.

[3] Cheng, C.Z. 1997 *J. Korean Phys. Soc. (Proc. Suppl.)* **31**, S128.

[4] Cuperman, S., Bruma, C. and Komoshvili, K. 2003 *J. Plasma Phys.*, **69**, 15.

[5] Fu, Y.G. and Van Dam, J.W. 1989 *Phys. Fluids B*, **1**, 1949.

[6] Sykes, A. 1994 *Plasma Phys Contr. Fusion* **36**, B93.

[7] Wilson, H.R. 1994 "SCENE—Simulation of Self-Consistent Equilibria with Neoclassical Effects", *Fusion Theoretical and Strategic Studies Depart.*, Culham Laboratory, Abingdon, UK.